Supercritical Swelling of Liquid Crystal Films

John M. O' Callaghan, Mark P. Copley, John P. Hanrahan, Michael A. Morris, David C. Steytler[#], Richard K. Heenan[†], Reiner Staudt[§] and Justin D. Holmes[*]

Department of Chemistry, Material Section and Supercritical Fluid Centre, University College Cork, Cork, Ireland and Centre for Research on Adaptive Nanostructures and Nanodevices (CRANN), Trinity College Dublin, Dublin, Ireland. [#]School of Chemical Sciences and Pharmacy, University of East Anglia, Norwich, NR4 7TJ, UK. [†]ISIS-CLRC, Rutherford Appleton Laboratory, Chilton, Oxfordshire, OX110QX,UK. [§]Institute of Non-Classical Chemistry at the University of Leipzig, Permoserstr. 15, D-4318 Leipzig, Germany.

** To whom correspondence should be addressed: Tel: +353(0)21 4903301; Fax: +353 (0)21 4274097; E-mail: j.holmes@ucc.ie*

Abstract

The influence of liquid and supercritical carbon dioxide and liquid propane on the structural properties of both ionic and non-ionic surfactant-based liquid crystal films is discussed in this paper. Swelling of the films, measured using *in-situ* small angle neutron scattering (SANS), was found to be dependent on the solubility of the propane/carbon dioxide in the micelles of the respective liquid crystals. Additionally, under certain pressure conditions the structural properties of some of the films were

observed to change, ultimately leading to a loss of order in the micellar arrays of the liquid crystals.

Introduction

Investigation of polymeric liquid crystals (LCs) and their applications has become an important research area, with chemists exploiting the supramolecular ordering of LCs to create nanoscale materials. Of particular importance is LC templating of nanoporous materials, such as the mesoporous silicates MCM [1, 2], SBA [3] and MSU [4]. Ionic surfactants and non-ionic polymer LC templates are used in the synthesis of high quality mesostructured materials due to their supramolecular templating ability [5]. Many authors have reported the successful use of short chain ethylene oxide surfactants [6] and triblock copolymer surfactants containing poly(ethylene oxide) (PEO) and poly(propylene oxide) (PPO) segments [3, 7-9] in the synthesis of mesoporous materials.

LCs also have the ability to absorb significant amounts of solvent and consequently swell [10, 11]. However conventional swelling of LC templates with non-polar solvents requires careful consideration of many factors including the ionic strength of the solvent when swelling ionic surfactants, pH, temperature and the use a co-surfactant. To successfully swell the hexagonal phase of sodium dodecyl sulphate (SDS) Ramos *et al* [12] had to monitor the oil content of the LC solution and ionic strength of the swelling solvent and use a co-surfactant. In the study by Nagarajan *et al.* [13] swelling Pluronic aggregates with hydrocarbons resulted in cylinder to rod to lamellae micelle shape transitions.

Swollen liquid crystals (SLCs) have been utilized as templates for materials such as zirconia nanoneedles [14] and platinum nanoparticles [15] which were synthesised using sodium dodecyl sulfate SLCs, swollen with cyclohexane. In all cases the LC can easily be removed from the final material by destabilizing the SLC and washing with solvents. Work by Dos Santos and coworkers [16] has demonstrated the stability and dexterity of SLC templates over a wide range of pH values and compositions. Additionally, Yusuf *et al.* have utilized low molecular weight LCs to swell polymer thin films [11]. The researchers reported swelling of polymer thin films (approximately 150 μm thick) using low molecular weight LCs such as 4-*n*-pentyl-4-cyanobiphenyl and 4-methoxy-benzilidene-4-butyl-aniline [11]. They showed that upon swelling of films that their crystalline nature and structure was retained. Hanrahan *et al.* have demonstrated that supercritical carbon dioxide (sc-CO_2) can be utilised to swell LC templates during the production of mesoporous silica materials [17, 18].

Lubeck *et al.* used Brij 97 LCs as a template to produce CdS nanostructures [19] and Karanikolos *et al.* used a LC templated from P105 to direct the formation of ZnSe nanostructures [20]. By swelling the LCs, ZnSe nanomaterials with a variety of sizes could be produced. Alexandrisdis [21] *et al* demonstrated swelling of up to 20 % of Pluronic LCs templated form P105 using glycols.

In this paper we characterise the swelling of both ionic and non-ionic surfactants LC films with sc-CO_2 and high density propane. Structural changes of the micelles in the LCs were investigated using small angle neutron scattering (SANS) as a function of pressure and temperature. It was found that swelling (increasing the distance between hexagonal rods) with sc-CO_2 was easily achieved without any loss of ordering, *i.e.* no

cylinder "wandering" was observed, as apposed to when conventional solvent swelling techniques are used. However, when propane was used to swell the same LCs problems such as structural rearrangements of the LCs at high propane pressures were encountered. The surfactants F127 [18], P123 [18], P85 [18], Brij 56 [22] and CTAB [23] at the concentrations used in this work have all been observed in the hexagonal phase in either LC experiments or as templates in mesoporous silica synthesis.

Experimental

Materials and Reagents. Hexadecyltrimethyl ammonium bromide (CTAB) (Fluka, UK) and F127 ($PEO_{100}PPO_{65}PEO_{100}$), P123 ($PEO_{20}PPO_{65}PEO_{20}$) and P85 ($PEO_{26}PPO_{40}PEO_{26}$), all polyethylene oxide-polypropylene oxide- polyethylene oxide triblock copolymers were used as received (BASF, New Jersey, U.S.A.). Deuterium (D_2O) and Brij 56 ($CH_3(CH_2)_{11}EO$) were used as supplied by Sigma-Aldrich. All surfactants used in this work can be found in table 1.

SANS Measurements of Liquid Crystal. *In-situ* high pressure SANS experiments were conducted on the LOQ instrument at ISIS at the Rutherford Appleton Laboratory (RAL) in Oxfordshire, UK. The absolute scattering cross-section I (Q) (cm^{-1}) was measured as a function of the modulus of momentum transfer $Q(A^{-1}) = (4\pi/\lambda)\sin(\theta/2)$ where λ is the incident neutron wavelength (2.2 to 10 Å) and θ is the scattering angle (< 7°). All measurements were conducted at 40 °C. High pressure SANS measurements were made using the UEA high pressure cell described in detail elsewhere [28]. Measurements performed on tertiary surfactant/D_2O/CO_2 mixtures were conducted at co-aqueous surfactant concentrations of 50 wt%.

A stock solution of LC, which consisted of 50 wt% surfactant (either F127, Brij 56 or CTAB) in D_2O, was prepared 2 hr before SANS measurements were undertaken. The surfactant was dissolved in the D_2O while stirring at room temperature. The resultant viscous LC paste was applied evenly to the sapphire entrance window of the pressure cell. In order to prevent the dehydration of the LC film a pad of cotton wool soaked in D_2O was inserted into the cell to saturate the CO_2 with water. The cell was allowed to equilibrate in both temperature and pressure for up to 30 min before SANS data was collected.

SANS data from the surfactant LC phase was consistent with the formation of a single pore size suggesting uniform dispersion of the copolymers within the cylindrical micelles which make up the hexagonal LC phases. The d-spacing (pore-centre-pore-centre distance, d) can be calculated using equation (1) [18] below:

$$d = \frac{4\pi}{Q_{MAX}\sqrt{3}} \qquad \textbf{(1)}$$

where Q_{Max} is the position of the diffraction peak maximum.

Model for swelling of Liquid Crystals. A simple model based on volume and surface area considerations was used to describe and understand the swelling of the LC phases. The model considers an initial volume of the LC phase (before swelling) filled with a number (n_1) of hexagonally arranged cylindrical micelles with fixed core radius r_1 and volume V_{P1}. This square slab is assumed to expand laterally but have fixed height. After swelling with CO_2 conservation of PPO:PEO interfacial area will dictate that the sample volume contains a reduced number of LC micelles (n_2) with

radius r_2 and PPO core (plus CO_2) volume V_{P2}. Equations (2) and (3) follow from this approach.

$$\frac{V_{P2}}{V_{P1}} = \frac{n_2 r_2^2}{n_1 r_1^2} \quad \textbf{(2)}$$

$$\frac{A_{S2}}{A_{S1}} = \frac{n_2 r_2}{n_1 r_1} \quad \textbf{(3)}$$

Where A_{S1} and A_{S2} are the mean area occupied by one surfactant molecule at the core-shell interface. Making the assumption that $A_{S1}=A_{S2}$, equations (2) and (3) yield equation (4) below:

$$\frac{V_{P2}}{V_{P1}} = \frac{r_2}{r_1} \quad \textbf{(4)}$$

The Pluronic LC d-spacing (D) changes through two effects, firstly an expansion in area of the slab as shown in equation (5),

$$d \propto a^{1/2} \propto (V_W + V_E + V_P)^{1/2} \quad \textbf{(5)}$$

Where V_W = volume of water (V_{W1} is before swelling and V_{W2} is after swelling), V_E = volume of PEO (it is assumed that the PEO micelle corona dimensions do not change), V_P = volume of PPO (V_{P1} before swelling and V_{P2} after swelling)

Secondly, as a requirement that $A_{S1}=A_{S2}$, the number of micelle cylinders n will decrease as $n \propto (1/r)$. This rearrangement will result in changes in an increase in d-spacing according to $d \propto (1/n)^{1/2}$. The overall result is that $d \propto r^{1/2}$ and since $r \propto V_P$ we obtain equation (6) below:

$$d \propto V_P^{1/2} \tag{6}$$

The combined swelling given by (5) and (6) can be written as shown in equation (7),

$$\frac{d_2}{d_1} = \left(\frac{V_{W2} + V_E + V_{P2}}{V_{W1} + V_E + V_{P1}} \right)^{1/2} \left(\frac{V_{P2}}{V_{P1}} \right)^{1/2} \tag{7}$$

Both the water (W) and PPO pseudo phases can be swollen by CO_2 and hence the above can be re-written in a form where the d-spacing increase with swelling (S) is given by,

$$\frac{d_S}{d} = \sqrt{S_{PO} \frac{V_{EO} + V_W S_W + V_{PO} S_{PO}}{V_{EO} + V_W + V_{PO}}} \tag{8}$$

where d_S represents the d-spacing of the swollen (S) phase and d that of the non-swollen phase. This allows the swelling contributions of the PPO core and aqueous phase (W) to be expressed in terms of volume fractions ϕ_{CO_2-PPO} and ϕ_{CO_2-W} respectively as $S_{PO} = 1 + \phi_{CO_2-PO}$ and $S_W = 1 + \phi_{CO_2-W}$.

If expansion of interfacial area is allowed the above expression becomes (equation (9)):

$$\frac{d_S}{d} = \left(\frac{A_{S1}}{A_{S2}}\right)\sqrt{S_{PO}\frac{V_{EO} + V_W S_W + V_{PO} S_{PO}}{V_{EO} + V_W + V_{PO}}} \qquad \textbf{(9)}$$

Here the maximum value of (A_{S1}/A_{S2}), corresponds to swelling with no increase in micelle number ($n_1 = n_2$) is $S_{PO}^{-0.5}$.

Liquid Crystal Solubility measurements. CO_2 adsorption measurements were performed on a magnetic suspension balance, Rubotherm (Bochum, Germany). This method measures the change of weight of a sorbent due to adsorption of molecules from a surrounding compressed gas phase. The balance can be operated up to 500 bar using a magnetic coupling concept, which isolates the interior of the balance and the surrounding immediate environment. The weight gained by the substance is transmitted by magnetic suspension coupling from a closed and pressure-proof metal container to an external microbalance.

Results and Discussion

Figures 1 (a), (b) and (c) illustrate the effect of liquid CO_2 and sc-CO_2 pressure on the d-spacing of 50 wt% LC micelles of the Pluronic surfactant F127, the non-ionic surfactant Brij 56 and the ionic surfactant CTAB respectively as measured by SANS. The determination of structural arrangement of micelles was not the concern of this work and to identify the correct micelle packing would require further structural analysis of these systems. With increasing liquid CO_2 and sc-CO_2 pressure the d-spacing of the LC film micelles increases, as observed by the shift of Q_{max} to lower Q values. Since the swelling of the aqueous phase is minimal ($S_W = 1 + \phi_{CO_2-W} \cong 1$) this increase in the d-spacing can be attributed solely to an increase in the micelle-to-micelle distance as the volume of the micelles swells with the uptake of liquid CO_2 and sc-CO_2, see figure 2. The corresponding increase in d-spacing obtained by application of equation 1 to the SANS data of figure 1 is shown as a function of sc-CO_2 pressure in figure 3.

The initial swelling of the F127 LC in both liquid CO_2 and sc-CO_2 shows a d-spacing increase from 175 Å to 203 Å upon increasing the pressure from 1 to 100 bar respectively, corresponding to an increase of 16 %. However, the increase in the d-spacing from 100 to 500 bar is very small, only 1 % of the overall swelling. The majority of the swelling takes place before 100 bar which is consistent with data reported for other Pluronic systems pressurised under sc-CO_2 [18]. This trend in the Pluronic LC swelling was also seen when the solubility of CO_2 in the 50 wt% LC of the Pluronic triblock copolymer P123 ($PEO_{20}PPO_{70}PEO_{20}$) was investigated by mass balance measurements, see figure 4. An increase in the solubility of CO_2 in the P123 LC is observed with increasing pressure. This increased CO_2 uptake is seen up to a

maximum at 100 bar, after which time the solubility is seen to level out. This result corresponds well with the SANS data obtained for the F127 LC and P123 LC data previously reported [18] and indicates that the solubility of the fluid in the surfactant causes the swelling.

The ability of CO_2 to swell the F127 micelle is due to the chemical composition of the micelle [24]. As with hydrocarbon solubilisation, CO_2 will predominantly dissolve in the polypropylene oxide (PPO) core of the micelles where the extent of solubilisation, and hence swelling of the LCs, increases with pressure.

The model used to obtain equation 8 links the d-spacing with the increase in micelle size as a function of CO_2 uptake. Using this approach, the radius of the Pluronic P123 LC micelle core was predicted for a number of pressures. These data are shown in figure 5 along with other calculated physical parameters of the P123 LC micelles under sc-CO_2 pressure. These data are presented as physical dimensions (Å) plotted against the PPO swelling factor (S_{PPO}) which is representative of the volume fraction of CO_2 taken up by the micelle core. Of course the micelle uptake of CO_2 depends on the pressure of CO_2. Also shown in figure 5 is the d-spacing and corresponding "wall thickness", *i.e.* the distance between corresponding micelle cores. Using pore size BJH calculations from calcined mesoporous silica synthesised using the P123 surfactant under sc-CO_2 from previous work [18], and taking into account calcination contraction ($\approx$ 30 % [25]), the simple model predicts changes in dimensions of the CO_2-swollen LC phase of similar magnitude to those obtained from experimental measurements.

Since the CO_2 swells the PPO core of the micelles, the percentage PPO present in the liquid crystal micelle influences the increase in d-spacing. A greater extent of micelle expansion is seen in those Pluronic surfactants with a higher ratio of PPO to PEO. This is illustrated in figure 6 for the three Pluronics examined F127 (19 %) < P85 (25 %) < P123 (45 %) where the % of PPO to PEO blocks is given in brackets. However, application of the swelling model, with a conserved surfactant head group area, gives values for ϕ_{CO_2-PPO} as F127 (0.17) < P85 (0.25) < P123 (0.30). This would imply that CO_2 uptake by PPO declines with increasing EO number of the Pluronics. However, this is out of step with the general observation of a decreasing uptake with increasing molecular weight for liquids and polymers. An alternative explanation is that the head group area is not conserved but increases to a greater extent with increasing EO number. For this approach reasonable agreement is obtained for a constant ϕ_{CO_2-PPO} = 0.32 and the extent of head group expansion (A_{S2} / A_{S1}) as F127 (1.15) < P85 (1.02) < P123 (1.0). Here F127 and P123 represent the extremes of maximum and minimum area expansion at the interface respectively.

Both the Brij 56 (figure 1b) and CTAB (figure 1c) LCs also show a significant shift of Q_{max} with increasing sc-CO_2 pressure. Swelling of the Brij 56 and CTAB LCs resulted in an increase in the d-spacing of these films by 14.6 % and 5.6 % respectively.

The swelling of LCs with alkyl chain hydrophobes can be partly explained by considering the solubility of CO_2 in different n-alkanes. The uptake of sc-CO_2 has previously been reported to decrease as the length of the alkane chain increases [26]. However, as the Brij 56 (C_{16}) and CTAB (C_{16}) micellar cores have the same

composition, the extent of swelling should to be the same. However, when the structures of the CTAB and Brij 56 micelles are compared it is then reasonable to assume that the larger PEO units of the Brij 56 micelles affect the spacing between neighbouring micelles to such an extent that the distance between micelles is increased. This is mirrored in the swelling of Brij 56 and CTAB LCs by sc-CO_2. Interestingly, the swelling plateau observed for the F127 LC in sc-CO_2 is also seen in the Brij 56 and CTAB LCs; see figure 3.

The change in d-spacing at constant pressure (200 bar) with varying temperature for the F127 LC is shown in figure 7. At 200 bar the d-spacing is approximately 175 Å, which corresponds to the d-spacing shown in figure 3 of the F127 LC at atmospheric pressure. An increase in the d-spacing does not occur until the temperature approaches the critical temperature (T_c) of CO_2 (31.3 °C, the critical pressure of CO_2 is 74 bar). Once the T_c of CO_2 is reached the viscosity and surface tension of the CO_2 atmosphere is reduced drastically and sc-CO_2 is able to penetrate into the highly viscous LC film, where the liquid CO_2 at low temperature was unable to do so.

As stated above the F127 LC is composed of a hydrophobic PPO micelle core and a hydrophilic PEO corona/interface [13, 24, 27]. It is the CO_2 – ether interactions that makes CO_2 so soluble in the PPO core [28] and it is the unique properties of sc-CO_2 [18] that improves its uptake of CO_2 into the micelles, as seen by inactive swelling below T_C. A degree of polarity is also important for CO_2 uptake, which is present in the PPO block but lacking in the PEO block [29]. The solubility of CO_2 in any polymer system can be explained by the plasticisation effect of CO_2 on the polymer. At increased pressure, gas molecules are forced between the polymer chains and expand the

spacing between the polymer chains which increases mobility. This results in more gas molecules being absorbed within the chains when the gas pressure is increased [30].

It is not thought that the "schizophrenic" nature, *i.e.* density fluctuations between CO_2 in the gas phase and CO_2 in the liquid phase and the tendency of CO_2 to prefer either gas or liquid at near critical conditions, is of concern in this work due to the fact that measurements were not conducted around the critical point of CO_2. Measurements were conducted above and below the critical point. A detailed swelling study around the critical points of CO_2 may illustrate anomalous swelling and/or CO_2 uptake due to density fluctuation domains.

Also shown in figure 7 is the F127 LC under the same temperature profile but in the absence of CO_2; no change in the micelle size was observed. Figure 7 also shows the d-spacing of a 50 wt% F127 LC at constant propane pressure with increasing temperature. However, the critical temperature of propane (96.7 °C) was not reached during this experiment and no similar change of d-spacing, as seen in the F127 liquid crystal in CO_2, was observed.

Figures 8 (a), (b) and (c) show how Q_{max} for the 50 wt% Pluronic surfactants F127, the non-ionic surfactant Brij 56 and the ionic surfactant CTAB LCs change as a function of propane pressure, respectively. From the scattering pattern shown in figure 8 (a) it is clear that propane has no affect on the F127 LC micelles since there is no real change in the d-spacing (figure 9). King *et al.* [31] has previously reported that propane uptake decreases with increasing polymer size and since F127 is heavier than

those polymer surfactants studied, the lack of swelling can be attributed to the low solubility of propane in the relatively heavier tri-block copolymer F127 [31].

In contrast Q_{max} was observed to decrease with increasing propane pressure for both the 50 wt% CTAB and Brij 56-templated LCs, indicating an increase in d-spacing. However, at high pressure both of these LC templates appear to be either destabilized or change morphology, as shown in figures 8 (b) and (c). In the case of Brij 56, Q_{max} was observed to split into two separate peaks and lose its intensity above a propane pressure of 200 bar. However, when the pressure was reduced below 200 bar the peak was stable. This peak splitting may be the result of a change in morphology, possibly from hexagonally-ordered micellar cylinders to an unidentified arrangement of micelles, at high propane pressures.

Shown in figure 8 (c), prior to the destabilization of the CTAB LC by propane, is a very intense Q_{Max} peak at approximately 0.084 $Å^{-1}$ (d-Spacing = 85 Å), up to a pressure of approximately 300 bar. Above this pressure Q_{Max} drastically loses intensity and peak shape, but regains both when the pressure is returned to below 300 bar. Figure 9 shows the changes in d-spacing in F127, Brij 56 and CTAB LCs with increasing propane pressure before their destabilization.

The differences observed in the extent of swelling of the CTAB LCs when sc-CO_2 and propane gas were used as swelling agents, is indicative of the solubility of sc-CO_2 and propane gas in the CTAB LCs. Swelling the CTAB LCs at 300 bar in sc-CO_2 gives a 5.5 % increase in d-spacing, compared with an 11 % increase in the d-spacing at the same pressure for propane. The ability of propane to swell the CTAB LC to a

greater extent may be explained by propane's higher solubility in the long chain alkane core of the CTAB micelles.

This increased solubility of propane, compared to CO_2, in CTAB seems to be in agreement to that reported by Roy and co-workers [32], who investigated the solubility of propane and CO_2 in low concentrations of CTAB and sodium dodecyl sulphate (SDS) solutions. At the CTAB concentrations used in this work the solubility of propane in CTAB would be greater than that of CO_2 in CTAB.

In the case of the Brij 56 LCs swelled by propane, it was shown by Beckman *et al.*, who studied the effect of liquid propane and ethane pressures on the structure of Brij 52 and Brij 30 microemulsions, that as the pressure of propane increases, the affinity of propane to the alkane tail of the Brij surfactants [33]. For this reason we see the initial swelling of Brij 56 by propane.

Conclusions

The data presented here demonstrates that surfactant LC films can be readily swollen in liquid carbon dioxide, supercritical carbon dioxide and liquid propane solvents. SANS data showed that the structural changes and swelling of the LCs was dependent on the solubility of the gases (propane or CO_2) in the respective micelles of the LCs. Modelling of the data showed that the micelle diameter increased with increasing CO_2 pressure, results in an increase in the observed d-spacing of the LCs. Differences were also seen in the stability of the LCs in a propane gas environment compared to CO_2. All the LCs were very stable in liquid CO_2 and sc-CO_2, however in a propane atmosphere some of them lost order or changed morphology, as observed by changes

in peak shape, peak splitting and a loss of intensity of Q_{max}. This work demonstrates the advantages of using sc-CO_2 over conventional swelling methods (hydrocarbon swelling) as the beneficial properties of CO_2 play an integral role in the swelling of the surfactant LCs.

Acknowledgements

The authors acknowledge financial support from the Centre for Research on Adaptive Nanostructures and Nanodevices (CRANN) (Project PR22) and from the European Community through its Access to Research Infrastructure action of the Improving Human Potential Programme.

References

(1). Kresge, C. T.; Leonwicz, M. E.; Roth, W. J.; Vartulli, J. C.; Beck, J. S., *Nature* **1992,** *359*, 710.

(2). Beck, J. S.; Vartulli, J. C.; Roth, W. J.; Leonowicz, M. E.; Kresge, C. T.; Schmitt, K. D.; Chu, C. T.; Olson, D. H.; Shepard, E.; McMyllen, S. B.; Higgins, J. B.; Schlenker, J. L., *J. Am. Chem. Soc.* **1992,** *114*, 10834.

(3). Zhao, D.; Feng, J.; Huo, Q.; Melosh, N.; Fredrickson, G. H.; Chmelka, B. F.; Stucky, G. D., *Science* **1998,** *279*, 548.

(4). Martines, M. A. U.; Yeong, E.; Larbot, A.; Prouzet, E., *Micro. Meso. Mater.* **2003,** *74*, 213.

(5). Flodstrom, K.; Alfredsson, *Micro. Meso. Mater.* **2003,** *59*, 167-179.

(6). Attard, G. S.; Glyde, J. C.; Goltner, C. G., *Nature* **1995,** *378*, 366.

(7). Huo, Q.; Margolese, D. L.; Ciesla, U.; Demuth, D. G.; Feng, P.; Gier, T. E.; Sieger, P.; Chmelka, B. F.; Schuth, F.; Stucky, G. D., *Chem. Mater.* **1994,** *6*, 1176.

(8). Huo, Q.; Margolese, D. L.; Stucky, G. D., *Chem. Mater.* **1996,** *8*, 1147.

(9). Zhao, D.; Sun, J.; Li, Q.; Stucky, G. D., *Chem. Mater.* **2000,** *12*, 275.

(10). Lee, J.; Choi, S.-U.; Yoon, M.-K.; Choi, Y. W., *Arch. Pharm. Res.* **2003,** *26*, 880.

(11). Yusuf, Y.; Ono, Y.; Sumisaki, Y.; Cladis, P. E.; Brand, H. R.; Finkelmann, H.; Kai, S., *Phys. Rev. B* **2004,** *69*, 4-10.

(12). Ramos, L.; Fabre, P., *Langmuir* **1997,** *13*, 682.

(13). Nagarajan, R., *Colloid Surface B* **1999,** *16*, 55.

(14). Dos Santos, E. P.; Santilli, C. V.; Pulcinelli, S. H.; Prouzet, E., *Chem. Mater.* **2004,** *16*, 4187-4192.

(15). Surrendran, G.; Tokumoto, M. S.; Pena dos Sontos, E.; Remita, H.; Ramos, L.; Kooyman, P. J.; Valentim Santilli, C.; Bourgaux, C.; Dieudonne, P.; Prouzet, E., *Chem. Mater.* **2005**, 1505.

(16). Dos Santos, E. P.; Tokumoto, M. S.; Surendran, G.; Remita, H.; Bourgaux, C.; Dieudonne, P.; Prouzet, E.; Ramos, L., *Langmuir* **2005,** *21*, 4362-4369.

(17). Hanrahan, J. P.; Copley, M. P.; Ryan, K. M.; Spalding, T. R.; Morris, M. A.; Holmes, J. D., *Chem. Mater.* **2004,** *16*, 424.

(18). Hanrahan, J. P.; Copley, M. P.; Ziegler, K. J.; Spalding, T. R.; Morris, M. A.; Steytler, D. C.; Heenan, R. K.; Schweins, R.; Holmes, J. D., *Langmuir* **2005,** *21*, 4163-4167.

(19). Lubeck, C. R.; Yong-Ying;, H. T.; Gash, A. E.; Sctcher, J. H. J.; Doyle, F. M., *Adv. Mater.* **2006,** *18*, 781.

(20). Karanikolos, G. N.; Alexandrisdis, P.; Mallory, R.; Petrou, A.; Mountziaria, T. J., *Nanotechnology* **2005,** *16*, 2372.

(21). Alexandrisdis, P.; Ivanova, R.; Lindman, B., *Langmuir* **2000,** *16*, 3676.

(22). El-Safty, S. A.; Hanaoka, T., *Chem. Mater.* **2003,** *15*, 2892.

(23). Coppola, L.; Gianferri, R.; Nicotera, I.; Oliviero, C.; Ranieri, G. A., *Phys. Chem. Chem. Phys.* **2004,** *6*, 2364.

(24). Lettow, J. S.; Lancaster, T. M.; Glinka, C. J.; Ying, J. Y., *Langmuir* **2005,** *21*, 5738.

(25). Raman, N. K.; Anderson, M. T.; Brinker, C. J., *Chem. Mater.* **1996,** *8*, 1682.

(26). Jha, S. K.; Madras, G., *Fluid Phase Equilibra* **2004,** *225*, 59-62.

(27). Sommer, C.; Pederson, J. S.; Garamus, V. M., *Langmuir* **2005,** *21*, 2137.

(28). Shen, Z.; McHugh, M. A.; Xu, J.; Belardi, J.; Kilic, S.; Mesoano, A.; Bane, S.; Karnikas, C.; Beckman, E.; Enick, R., *Polymer* **2003,** *44*, 1491.

(29). Rindfleisch, F.; DiNoia, T. P.; McHugh, M. A., *J. Phys. Chem.* **19996,** *100*, 15581.

(30). Aionicesei, E.; Skerget, M.; Knez, Z., *J. Chem. Eng. Data* **2008,** *53*, 185.

(31). King, A. D., *J. Colloid Interface Sci.* **2001,** *244*, 123.

(32). Roy, S.; Mehra, A.; Bhowmcik, D., *J. Colloid Interface Sci.* **1997,** *196*, 53.

(33). Beckman, E. J.; Smith, R. D., *J. Phys. Chem.* **1990,** *94*, 3729.

Figures

Table 1 The compositions of various surfactants used in this work

Surfactant	*Composition*
F127	$PEO_{100}PPO_{70}PEO_{100}$
P123	$PEO_{20}PPO_{70}PEO_{20}$
P85	$PEO_{20}PPO_{40}PEO_{20}$
CTAB	$(C_{16}H_{33})N(CH_3)_3$ Br
Brij 56	$(C_{16}H_{33})$ PEO_{10}

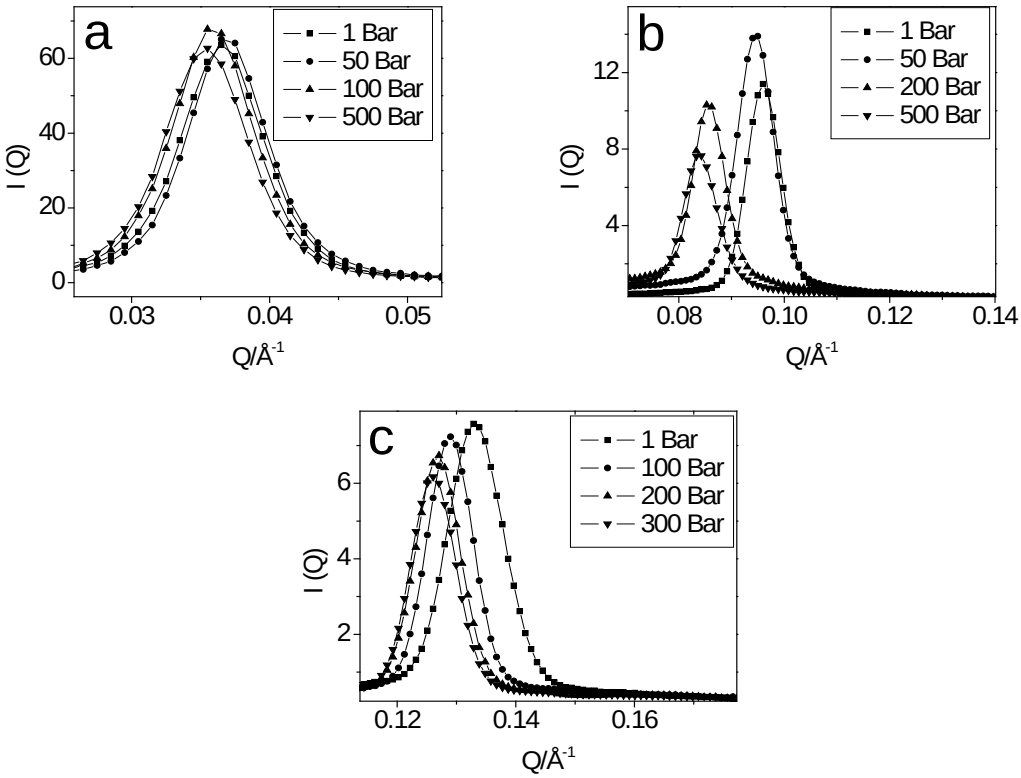

Figure 1 SANS scattering patterns observed for different surfactants in a sc-CO_2 atmosphere as a function of pressure and at constant temperature of 40 °C. (a), (b) and (c) show the effects of sc-CO_2 pressure on the F127, Brij 56 and CTAB LCs respectively. Each figure has a different scale for illustration purposes.

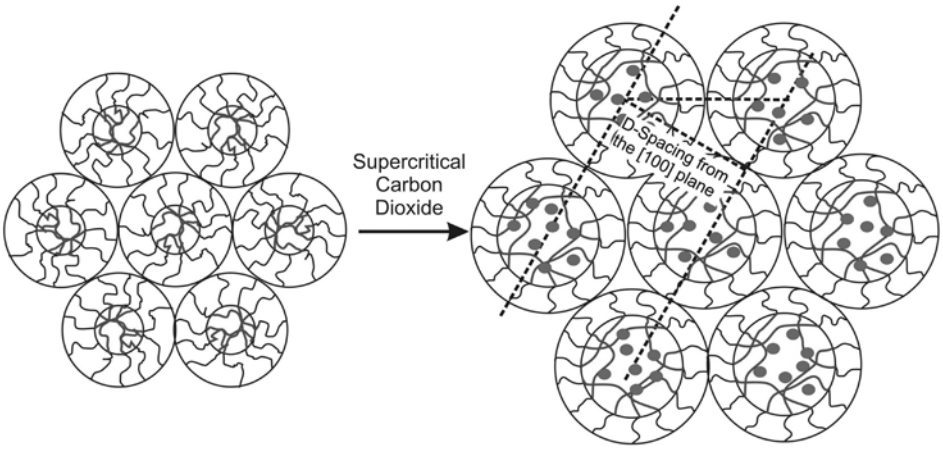

Figure 2 Schematic of the swelling process that takes place under an elevated sc-CO_2 pressure at a temperature of 40 °C.

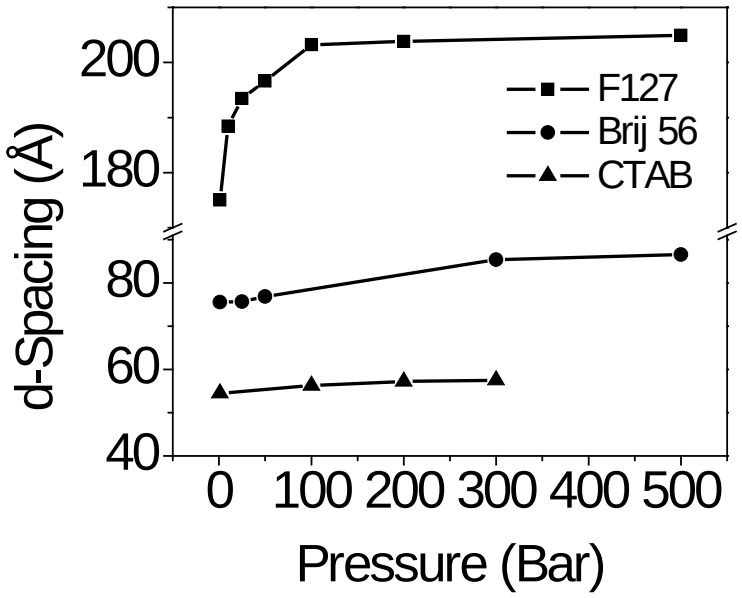

Figure 3 An overview of the structural changes observed in the LCs under a sc-CO_2 atmosphere as a function of pressure, at a constant temperature of 40 °C. Figure shows the changes in d-spacings of F127 (■), Brij 56 (●) and CTAB (▲) LCs in sc-CO_2.

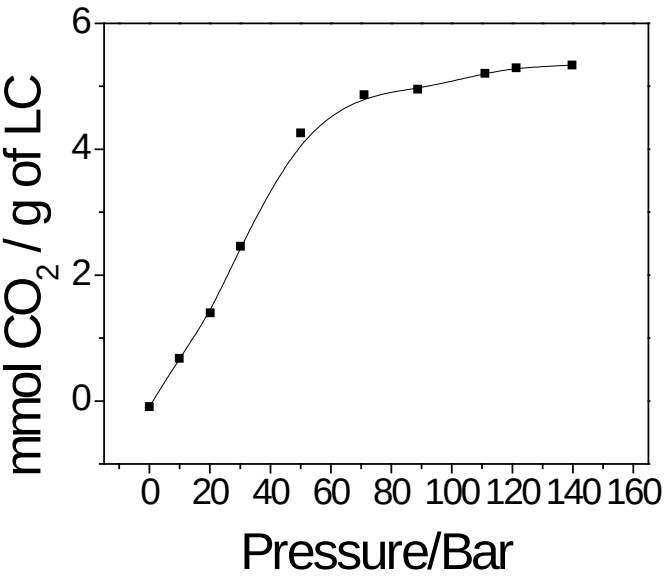

Figure 4 The adsorption of both liquid and sc-CO_2 in a P123 LC ($PEO_{20}PPO_{70}PEO_{20}$), determined by mass balance experiments conducted at a temperature of 40 °C.

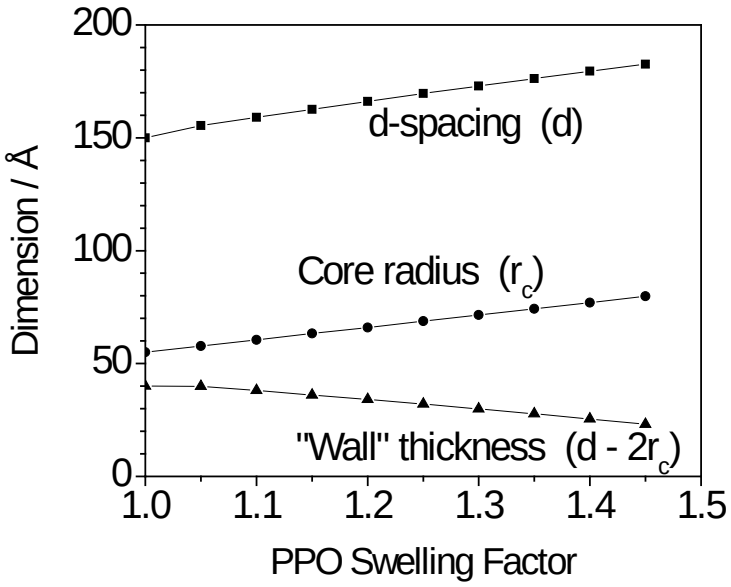

Figure 5 Physical parameters calculated from the SANS model (equation (9)) for the P123 LC micelles at a constant temperature of 40 °C. The PPO swelling factor scale depends on the size of the PPO micelle core.

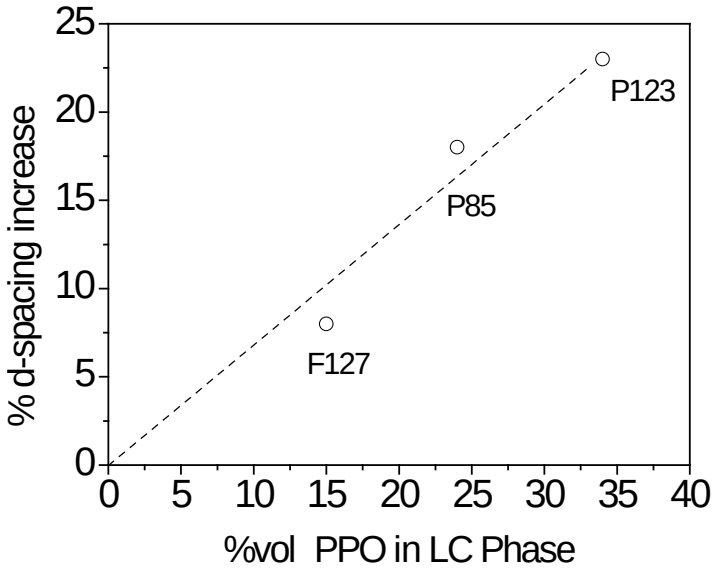

Figure 6 Degree of swelling in sc-CO_2 at a pressure of 500 bar and a temperature of 40 °C. The composition of each Pluronic is P123: $PEO_{20}PPO_{70}PEO_{20}$, F127: $PEO_{100}PPO_{70}PEO_{100}$ and P85: $PEO_{26}PPO_{40}PEO_{26}$.

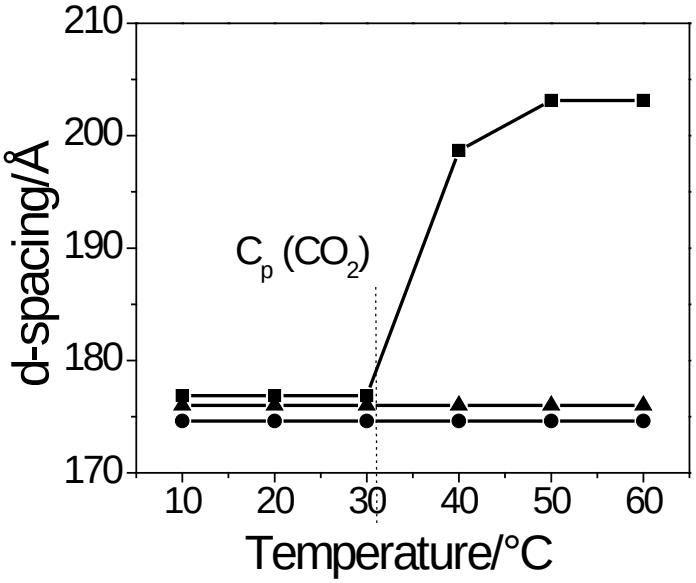

Figure 7 The influence of sc-CO_2 (■) and propane (●) on the d-spacing of the F127 LC as a function of temperature, at a constant pressure of 200 bar. Also shown (▲) is the change in d-spacing of the F127 LC at atmospheric pressure.

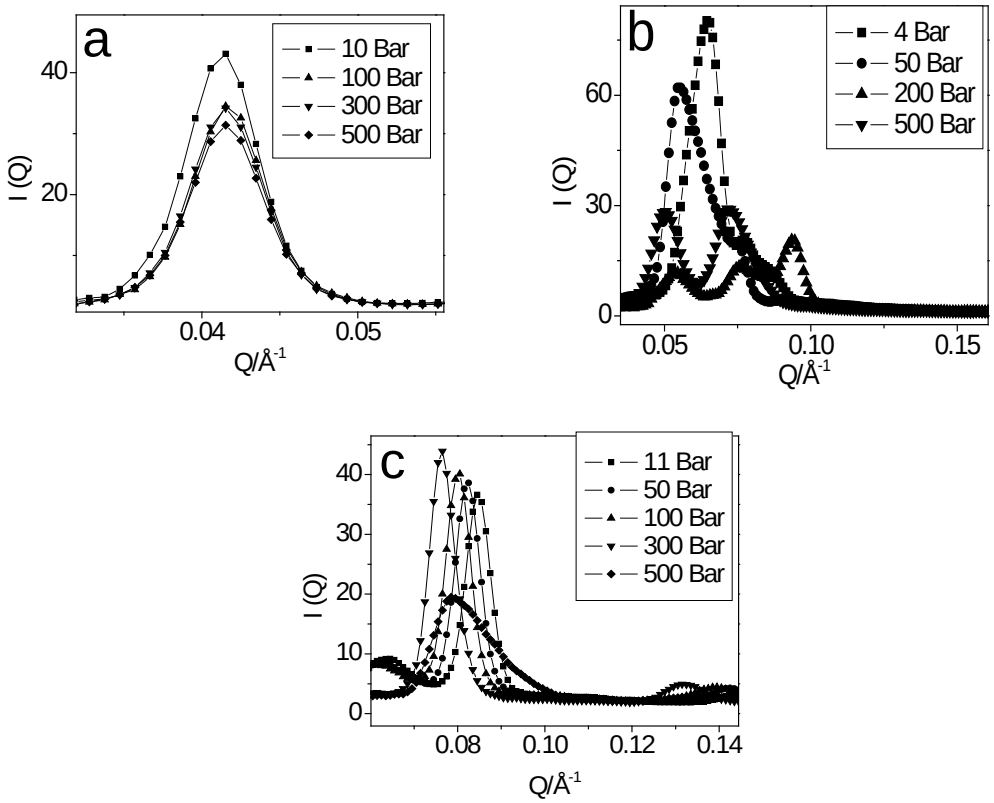

Figure 8 SANS scattering patterns observed for different surfactants in a propane atmosphere as a function of pressure, at a constant temperature of 40 °C. (a), (b) and (c) show the effects of propane pressure on the F127, Brij 56 and CTAB LCs respectively. Each figure has a different scale for illustration purposes.

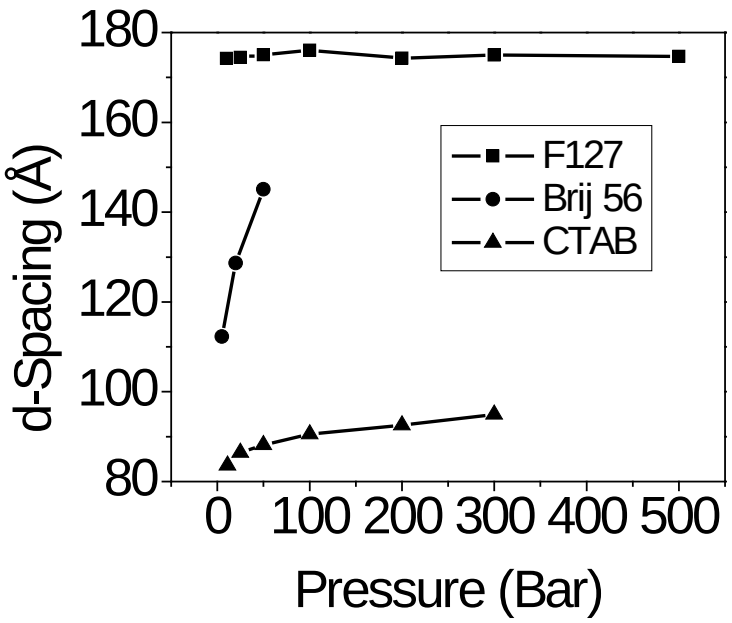

Figure 9 An overview of structural changes observed in LCs as a function of propane pressure, at a constant temperature of 40 °C. Figure shows the changes in d-spacings of F127 (■), Brij 56 (●) and CTAB (▲) LCs in propane.

Swelling of Liquid Crystal Films

John M. O' Callaghan, Mark P. Copley, John P. Hanrahan, Michael A. Morris, David C. Steytler, Richard K. Heenan, Reiner Staudt and Justin D. Holmes